The Thesis Committee for Nathan Gabriel Wu
Certifies that this is the approved version of the following thesis:

Sensitivity Calculations on a Soot Model Using a Partially Stirred Reactor

APPROVED BY

SUPERVISING COMMITTEE:

Venkatramanan Raman, Supervisor

Noel T. Clemens

Sensitivity Calculations on a Soot Model Using a Partially Stirred Reactor

by

Nathan Gabriel Wu, B.S.

THESIS

Presented to the Faculty of the Graduate School of
The University of Texas at Austin
in Partial Fulfillment
of the Requirements
for the Degree of

Master of Science in Engineering

THE UNIVERSITY OF TEXAS AT AUSTIN
May 2010

Dedicated to my parents for their continual love and support through difficult times.

Sensitivity Calculations on a Soot Model Using a Partially Stirred Reactor

Nathan Gabriel Wu, MSE
The University of Texas at Austin, 2010

Supervisor: Venkatramanan Raman

Sensitivity analysis was performed on a soot model using a partially stirred reactor (PaSR) in order to determine the effects of mixing model parameters on soot scalar values. The sensitivities of the mixture fraction ζ and progress variable C to the mixing model constant C_ϕ were calculated; these values were used to compute the sensitivity of water mass fraction Y_{H_2O} to C_ϕ and several soot quantities to soot moments. Results were validated by evaluating the mean mixture fraction sensitivity and a long simulation time case. From the baseline case, it was noted that soot moment sensitivities tended to peak on the rich side of the stoichiometric mixture fraction ζ_{st}. Timestep, number of notional particles, mixing timescale τ_{mix}, and residence time τ_{res} were varied independently. Choices for timestep and notional particle count were shown to be sufficient to capture relevant scalar profiles, and did not greatly affect sensitivity calculations. Altering τ_{mix} or τ_{res} was shown to affect sensitivity to mixing, and it was concluded that the soot model is more heavily influenced by the chemistry than mixing.

Table of Contents

List of Figures

Chapter 1

Introduction

Soot modeling is an important area of research due to the environmental and health concerns related to soot particles. Driven by the growing awareness in the public mind of such issues as global warming and the dangers of carcinogens, emissions standards placed on new engines are becoming more stringent. As such regulations come into play, the ability to accurately model and predict soot formation will contribute greatly towards the effective design of turbine and internal combustion engines [3][4].

Turbulence modeling is already highly complex, and adding the chemistry required to simulate combustion only serves to further complicate the matter. The complexity continues to increase when one attempts to factor in soot, as the means by which soot forms, interacts within the environment of a flame, and dissipates, is not yet fully understood [4].

In light of this matter, it is important to know how any soot model created behaves within a larger simulation with respect to the parameters of the overall simulation. Sensitivity analysis is conducted in order to quantify this behavior. Performing such an analysis on a full-scale combustion simulation is often impractical in the initial phase of model creation as it requires a large

amount of processing power and generally takes a long time to run [8]. Using a partially-stirred reactor (PaSR) model can significantly reduce computational costs due to its simplicity [7].

The objective of this study is to use a PaSR to understand how mixing model parameters, specifically the mixing model constant, influences the behavior of a soot model, and how this sensitivity is affected by various model input parameters.

Chapter 2

Theory and Methodology

2.1 The PaSR Model

Probability density function (PDF) methods are frequently used to overcome the source term closure problem that occurs in modeling turbulent combustion. However the PDF in such situations evolves in both physical and composition space, resulting in an N+4 dimensional transport equation, where N is the number of scalars considered in the thermo-chemical model.

The partially stirred reactor (PaSR) serves as a simplified test bed for this transport equation. First developed by Correa [1], the PaSR model has been previously used, among other things, to study mixing models [7] and in sensitivity analyses [8]. Flow within the reactor is considered spatially homogeneous, allowing the transport in composition space to be studied separately from the physical flow effects. The PaSR can be seen as representing one computational grid cell within a large PDF simulation.

A PaSR is a constant volume reactor containing a fixed number of notional particles, the ensemble of which represents the overall PDF. Each particle contains a set of scalars $\boldsymbol{\phi^{(n)}}$, representing for example species mass fractions and temperature. Also included in $\boldsymbol{\phi^{(n)}}$ is a weight w that denotes

the amount of the total fluid mass represented by the particle. The reactor has inflow from two inlet streams, one representing fuel and the other oxidizer, as well as an outlet stream. Total inflow and outflow rates are equal, resulting in a constant number of particles in the reactor, and thus a fixed fluid mass $\boldsymbol{m}$. This allows the mean residence time $\boldsymbol{\tau_{res}}$ to be defined as [7]

$$\boldsymbol{\tau_{res}} = \frac{\boldsymbol{m}}{\boldsymbol{\dot{m}}}, \tag{2.1}$$

where $\boldsymbol{\dot{m}}$ is the sum of the fuel and oxidizer mass inflow rates, or $\boldsymbol{\dot{m}_f}$ and $\boldsymbol{\dot{m}_o}$, respectively. Another useful variable to define is the mixture fraction $\boldsymbol{\zeta}$, which is given by [5]

$$\boldsymbol{\zeta} = \frac{\boldsymbol{\dot{m}_f}}{\boldsymbol{\dot{m}_f + \dot{m}_o}} \tag{2.2}$$

and which represents the fuel-to-oxidizer ratio.

If we consider the sample-space variable $\boldsymbol{\psi}$ corresponding to $\boldsymbol{\phi}$ and $\boldsymbol{\phi^0}$ and $\boldsymbol{\phi^1}$ as the compositions of the oxidizer and fuel inlet streams, respectively, and assume equal diffusivities $\boldsymbol{\Gamma}$, then the transport equation for the PDF $\boldsymbol{\tilde{P}}$ can be written [7]

$$\begin{aligned} \frac{\boldsymbol{\partial \tilde{P}}}{\boldsymbol{\partial t}} &= -\frac{\boldsymbol{\tilde{P}}}{\boldsymbol{\tau_{res}}} + \frac{\mathbf{1}}{\boldsymbol{\tau_{res}}}\left[\boldsymbol{\zeta}\delta(\boldsymbol{\phi^1} - \boldsymbol{\psi}) + (\mathbf{1} - \boldsymbol{\zeta})\delta(\boldsymbol{\phi^0} - \boldsymbol{\psi})\right] \\ &\quad -\frac{\boldsymbol{\partial}}{\boldsymbol{\partial \psi_\alpha}}\left[\boldsymbol{\tilde{P}}\left\langle \boldsymbol{\Gamma} \bigtriangledown^{\mathbf{2}} \boldsymbol{\phi_\alpha} | \boldsymbol{\psi} \right\rangle\right] - \frac{\boldsymbol{\partial}}{\boldsymbol{\partial \psi_\alpha}}\left[\boldsymbol{\tilde{P}} \boldsymbol{S_\alpha}(\boldsymbol{\psi})\right]. \end{aligned} \tag{2.3}$$

The first two terms in equation 2.3 represent the effects of outflow and inflow, respectively. As the common variable in both these two terms, $\boldsymbol{\tau_{res}}$ can be used to control the influence of fluid flow on the simulation. The third term denotes the influence of micro-scale mixing, and the final term represents the effects

of the reaction. With the source term provided directly from the chemistry mechanism, the only term requiring modeling is the mixing term.

2.1.1 The IEM Mixing Model

The interaction by exchange with the mean (IEM) mixing model serves as a simple method to approximate the mixing term in the PDF transport equation. The mixing term in equation 2.3 is modeled as

$$\left\langle \boldsymbol{\Gamma} \bigtriangledown^{\mathbf{2}} \boldsymbol{\phi_\alpha} | \boldsymbol{\psi} \right\rangle = -\frac{\mathbf{1}}{\mathbf{2}\boldsymbol{\tau_{mix}}} \left(\boldsymbol{\psi} - \tilde{\boldsymbol{\phi}} \right), \tag{2.4}$$

where $\tilde{\boldsymbol{\phi}}$ is the Favre-averaged (or filtered) composition of the ensemble. $\boldsymbol{\tau_{mix}}$ is the characteristic mixing timescale, and can be used to control the effects of mixing on the PaSR's content. The mixing timescale can be related to the characteristic turbulence timescale $\boldsymbol{\tau_t}$ by

$$\boldsymbol{\tau_t} = \boldsymbol{C_\phi \tau_{mix}}, \tag{2.5}$$

where $\boldsymbol{C_\phi}$ is the mixing model constant. In full scale simulations, $\boldsymbol{\tau_t}$ can be obtained from the turbulence model. $\boldsymbol{C_\phi}$ is not a universal constant. It depends upon various quantities including the scalar length scales; therefore it is important to understand the influence of $\boldsymbol{C_\phi}$ on simulation results.

2.1.2 Flamelet/Progress Variable Approach

The Flamelet/Progress Variable Approach (FPVA) was used to model combustion. In this model, scalars are mapped to a flamelet table based on mean mixture fraction $\tilde{\boldsymbol{\zeta}}$, mixture fraction variance $\widetilde{\boldsymbol{\zeta''^2}}$, and progress variable

$\tilde{\boldsymbol{C}}$. The progress variable $\boldsymbol{C}$ represents a linear combination of the major products of the reaction [2][6]. FPVA serves to greatly reduce the number of scalars stored by each particle. Instead of retaining information on each species present in the reaction, only $\tilde{\boldsymbol{\zeta}}$, $\widetilde{\boldsymbol{\zeta''^2}}$, and $\tilde{\boldsymbol{C}}$ are stored. When more detailed information is required, it can easily be looked up from the flamelet table.

2.2 Scalar Sensitivity

The evolution equation for the scalar composition $\boldsymbol{\phi^{(n)}}$ of the nth particle, using the IEM mixing model, is

$$\frac{\mathbf{d}\boldsymbol{\phi}_i^{(n)}}{\mathbf{d}\boldsymbol{t}} = \boldsymbol{S}_i(\boldsymbol{\phi}^{(n)}) + \frac{\boldsymbol{C}_\phi}{\boldsymbol{2\tau_t}}(\widetilde{\boldsymbol{\phi}_i} - \boldsymbol{\phi}_i^{(n)}). \tag{2.6}$$

The sensitivity vector $\boldsymbol{W}_i^{(n)}$ contains the sensitivities of the composition variables with respect to some input parameter. If we take this parameter to be $\boldsymbol{C}_\phi$, $\boldsymbol{W}_i^{(n)}$ becomes

$$\boldsymbol{W}_i^{(n)} = \frac{\boldsymbol{\partial\phi}_i^{(n)}}{\boldsymbol{\partial C}_\phi}. \tag{2.7}$$

The evolution of the sensitivity vector can thus be written as

$$\frac{\mathbf{d}\boldsymbol{W}_i^{(n)}}{\mathbf{d}\boldsymbol{t}} = \boldsymbol{J}_{ij}^{(n)}\boldsymbol{W}_j^{(n)} + \frac{\boldsymbol{\partial S}_i(\boldsymbol{\phi}^{(n)})}{\boldsymbol{\partial C}_\phi} + \frac{\boldsymbol{C}_\phi}{\boldsymbol{2\tau_t}}(\widetilde{\boldsymbol{W}_i} - \boldsymbol{W}_i^{(n)}) + \frac{\mathbf{1}}{\boldsymbol{2\tau_t}}(\widetilde{\boldsymbol{\phi}_i} - \boldsymbol{\phi}_i^{(n)}), \tag{2.8}$$

where the Jacobian matrix $\boldsymbol{J_{ij}}$ of the nth particle is given by

$$\boldsymbol{J}_{ij}^{(n)} \equiv \frac{\boldsymbol{\partial S}_i(\boldsymbol{\phi}^{(n)})}{\boldsymbol{\partial\phi}_j^{(n)}}.$$

For the case of sensitivity with respect to the mixing model constant, the second term in equation 2.8 is zero because the mixing model constant does not influence the source term.

2.2.1 Mixture Fraction and Progress Variable Sensitivity

Applying sensitivity analysis to the FPVA model, one becomes concerned only with the mixture fraction $\boldsymbol{\zeta}$ and progress variable $\boldsymbol{C}$. Thus the sensitivity vector can be written

$$\boldsymbol{W}_i^{(n)} = \begin{bmatrix} \frac{\partial \zeta}{\partial C_\phi} \\ \frac{\partial C}{\partial C_\phi} \end{bmatrix}.$$

Then the evolution equations for component sensitivities will be as follows:

$$\frac{\mathrm{d}}{\mathrm{d}t}\left(\frac{\partial \zeta^{(n)}}{\partial C_\phi}\right) = \frac{C_\phi}{2\tau_t}\left(\widetilde{\frac{\partial \zeta}{\partial C_\phi}} - \frac{\partial \zeta^{(n)}}{\partial C_\phi}\right) + \frac{1}{2\tau_t}(\widetilde{\zeta} - \zeta^{(n)}) \tag{2.9}$$

$$\frac{\mathrm{d}}{\mathrm{d}t}\left(\frac{\partial Y^{(n)}}{\partial C_\phi}\right) = \left[\left(\frac{\partial S_C^{(n)}}{\partial \zeta^{(n)}}\right)\left(\frac{\partial \zeta^{(n)}}{\partial C_\phi}\right) + \left(\frac{\partial S_C^{(n)}}{\partial C^{(n)}}\right)\left(\frac{\partial C^{(n)}}{\partial C_\phi}\right)\right] + \frac{C_\phi}{2\tau_t}\left(\widetilde{\frac{\partial C}{\partial C_\phi}} - \frac{\partial C^{(n)}}{\partial C_\phi}\right) + \frac{1}{2\tau_t}(\widetilde{C} - C^{(n)}) \tag{2.10}$$

For the $\boldsymbol{\zeta}$ sensitivity evolution equation, the first term of Equation 2.8 is zero because there is no mixture fraction source term.

2.3 Methodology

The PaSR simulation implemented tracked $\boldsymbol{\zeta}$, $\boldsymbol{C}$, other scalars pertaining to soot moments, and temperature, as well as the sensitivity of $\boldsymbol{\zeta}$, $\boldsymbol{C}$,

$\boldsymbol{Y_{H_2O}}$, and several soot quantities to $\boldsymbol{C_\phi}$. Each simulation timestep, the following steps occurred. First, reactor inflow and outflow were considered. A random number of particles from within the reactor were removed and replaced by particles set to the inlet stream compositions. Following this, a number of substeps based on $\boldsymbol{\tau_{mix}}$ were taken. During each substep, mean values were calculated, then a reaction half-step occurred during which the chemical source term was computed. This was followed by a mixing step, which was then followed by a second reaction half-step to end the substep sequence, as well as the simulation timestep. At certain intervals, mean composition values across the reactor were output to a file, particle scalar compositions to another, and particle sensitivity values to yet another before the inflow/outflow step was repeated. Soot was modeled using the Hybrid Method of Moments [3]. For the sensitivity calculations, differentiation was performed using the Double Precision Differential/Algebraic Sensitivity Analysis Code (DDASAC) algorithm.

Chapter 3

Results

3.1 Validation

In order to check the validity of the model, the mixture fraction sensitivity $\frac{\partial \zeta}{\partial C_\phi}$ was tracked throughout the duration of the simulation. Theory dictates that mean mixture fraction sensitivity should be zero, as mixture fraction is independent of the mixing model constant. Figure 3.1 shows that the time-averaged mean sensitivity was very close to the theoretical value. It was calculated to be -1.03e-004. The slight deviation below zero was due to unavoidable numerical errors.

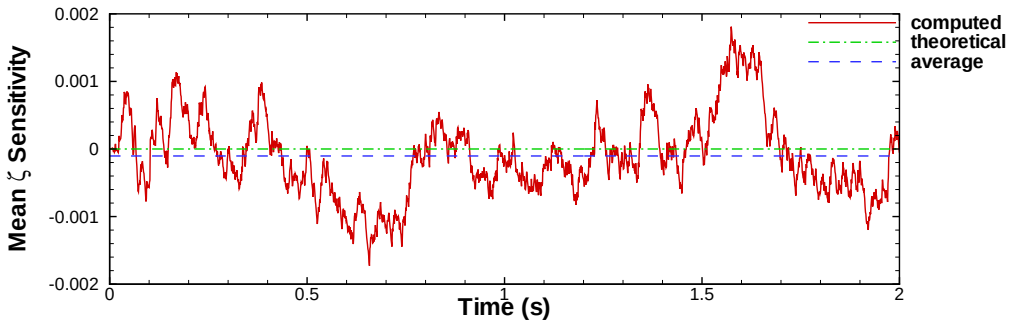

Figure 3.1: Mean Sensitivity of Mixture Fraction to C_ϕ over Time.

Additional validation was conducted by running a simulation to 20 seconds (as compared to the baseline duration of 2 seconds). Comparison of

the scalar quantities and sensitivities generally displayed very similar profiles, as seen in Figure 3.2.

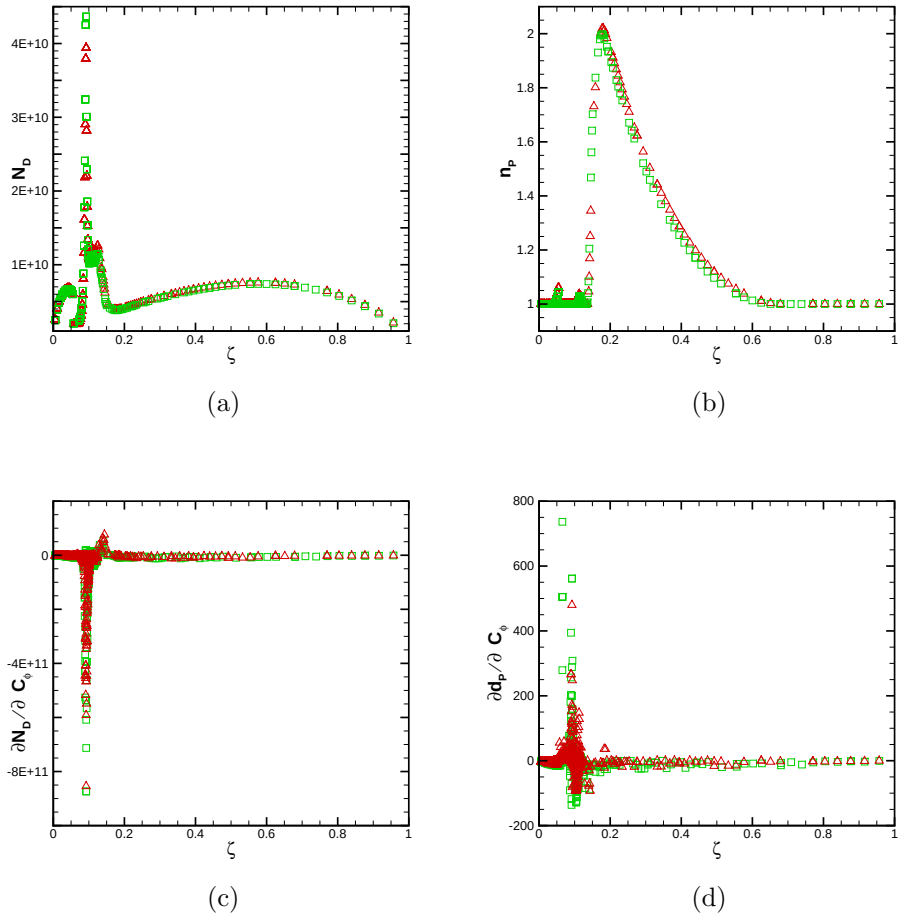

Figure 3.2: Scalar Quantities and Sensitivities at Different Time Durations: □ - 2 sec, △ - 20 sec

3.2 Baseline Case

The baseline case studied involved 1024 notional particles reacted for a total of 2 seconds simulation time with a timestep of 0.01 seconds, reaction timescale of 0.1, and mixing timescale of 0.02. $\boldsymbol{C_\phi}$ was held constant at a value of 2 for all calculations. Mixture fraction and progress variable were used to compute a temperature profile as well as four soot quantities: number density $\boldsymbol{N_D}$, volume fraction $\boldsymbol{F_V}$, diameter of the primary particle $\boldsymbol{d_P}$, and primary particle number $\boldsymbol{n_P}$. The sensitivity of the mixture fraction and progress variable to $\boldsymbol{C_\phi}$ were found as outlined in Section 2.2.1, and these values were used to calculate the water mass fraction sensitivity as well as the sensitivities of the soot quantities listed above to soot moments. Figure 3.3 shows the baseline profiles for the temperature and soot quantities against mixture fraction, and Figure 3.4 shows the sensitivity profiles for water mass fraction and soot quantities.

The dual-peaks in the water mass-fraction sensitivity plot (Figure 3.4a) are consistent with the results in [8]. These two peaks denote the fuel-lean and fuel-rich edges of the reaction zone.

A comparison of the scalars and sensitivities normalized to absolute maximum values reveals interesting similarities in curve shape between some variables. Soot volume fraction ($\boldsymbol{F_V}$) and primary particle diameter ($\boldsymbol{d_P}$) values rise and fall at very similar mixture fractions. This comparison is shown in Figure 3.5a.

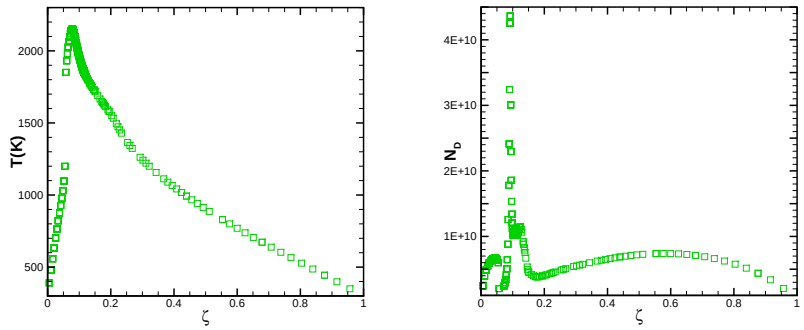

(a)

(b)

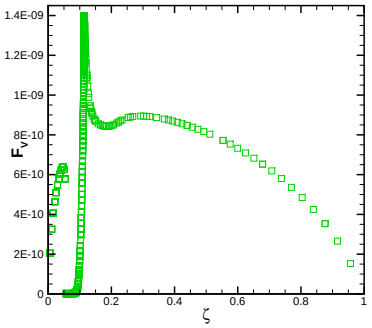

(c)

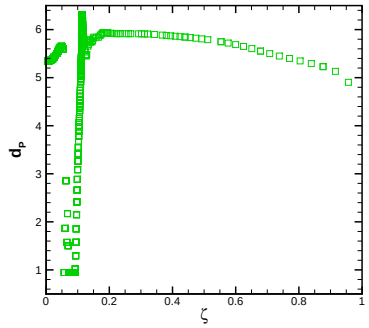

(d)

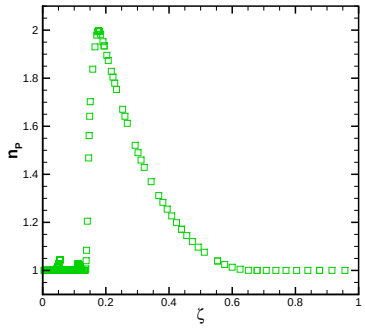

(e)

Figure 3.3: Baseline Scalar Profiles

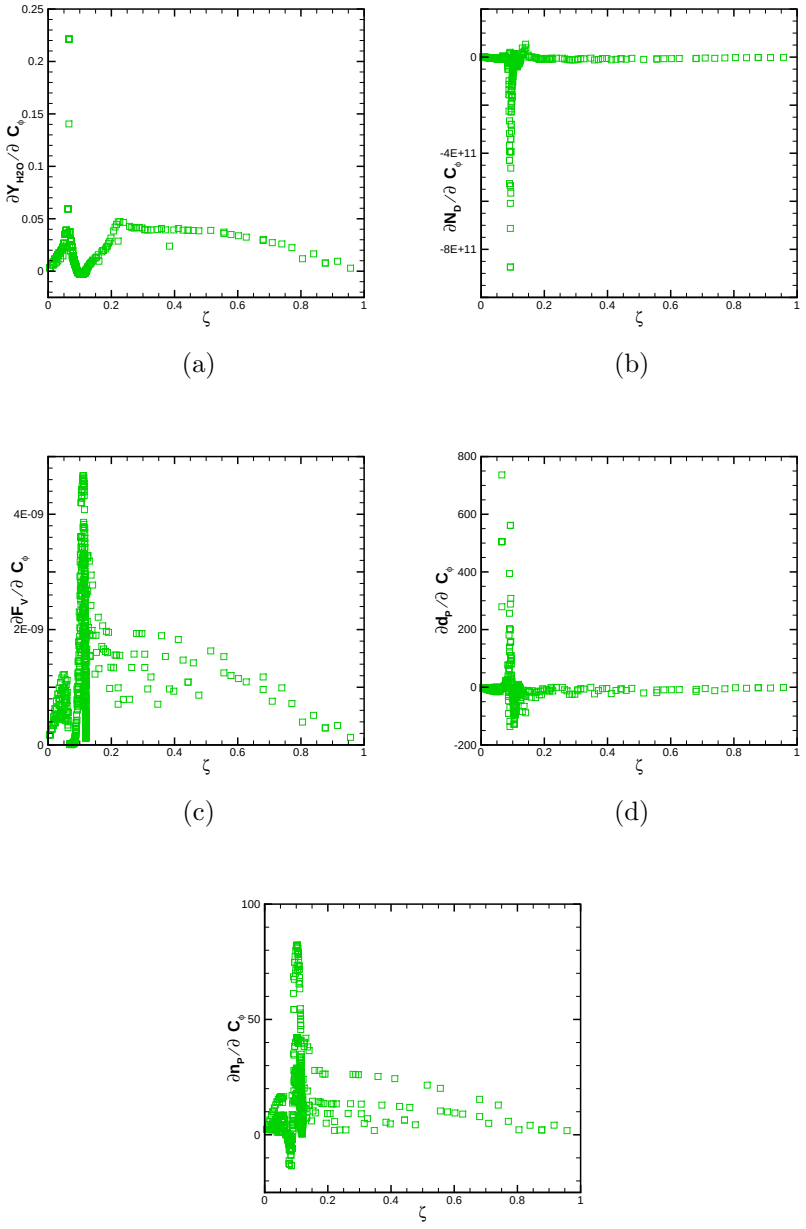

Figure 3.4: Baseline Sensitivity Profiles

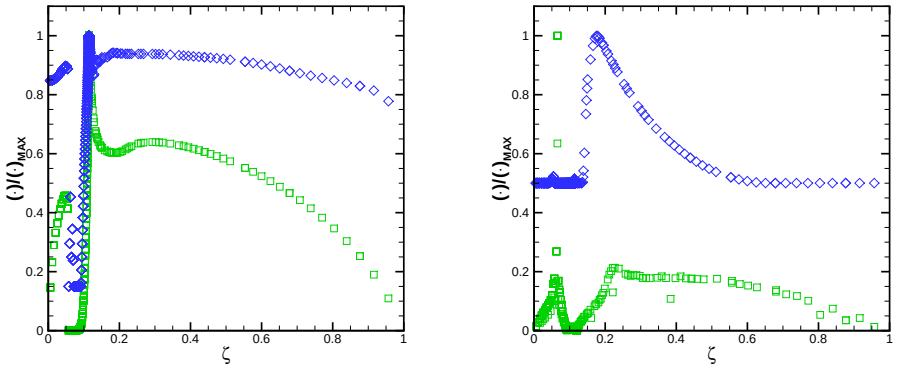

(a) (b)

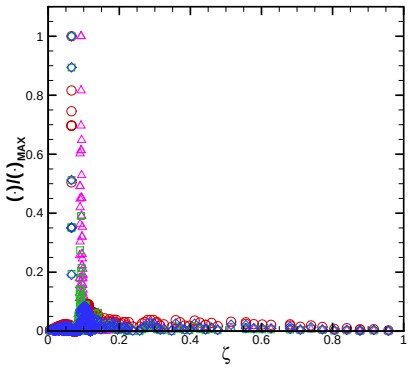

(c)

Figure 3.5: Comparisons of Normalized Values: (a)□ - $\boldsymbol{F_V}$ and ◇ - $\boldsymbol{d_P}$; (b)□ - $\boldsymbol{Y_{H_2O}}$ and ◇ - $\boldsymbol{n_P}$; (c) Soot Moment Sensitivity to $\boldsymbol{C_\phi}$

Additionally, some correlation is suggested between the fuel-rich boundary of the reaction zone and primary particle number $\boldsymbol{n_P}$. Plotting normalized curves of $\boldsymbol{n_P}$ and $\boldsymbol{Y_{H_2O}}$ sensitivity to $\boldsymbol{C_\phi}$ show that peak $\boldsymbol{n_P}$ values occur at roughly the same mixture fraction as the second peak in $\boldsymbol{Y_{H_2O}}$ sensitivity, as shown in Figure 3.5b.

Further, examination of the normalized soot moment sensitivities shows the majority of the sensitivity to be concentrated between mixture fraction values of 0.05 and 0.15. Figure 3.5c shows the sensitivity of $\boldsymbol{N_D}(\triangle)$, $\boldsymbol{F_V}$ $(\circ)$, $\boldsymbol{d_P}$ $(\square)$, and $\boldsymbol{n_P}$ $(\diamond)$ to $\boldsymbol{C_\phi}$. It can be noted that the largest sensitivity values are very near the stoichiometric mixture fraction $\boldsymbol{\zeta_{st}}$, which corresponds with the peak temperature in the $\boldsymbol{T}$ vs. $\boldsymbol{\zeta}$ plot (Figure 3.3a).

3.3 Input Parameter Sensitivities

The baseline case conditions were systematically adjusted in order to see the effects of input parameters on the scalar quantities and sensitivities. Timestep, total number of particles, mixing timescale, and residence time were independently altered, and the results compared to the baseline case. In the following figures, the baseline case is denoted with a green $\square$. Reduced input parameter cases use a red $\triangle$, and increased input parameter cases are marked by a blue $\diamond$.

3.3.1 Timestep

The baseline timestep of 0.01 seconds was increased and decreased by a factor of 10 in separate runs to see its effect on simulation output. Figure 3.6 shows these results.

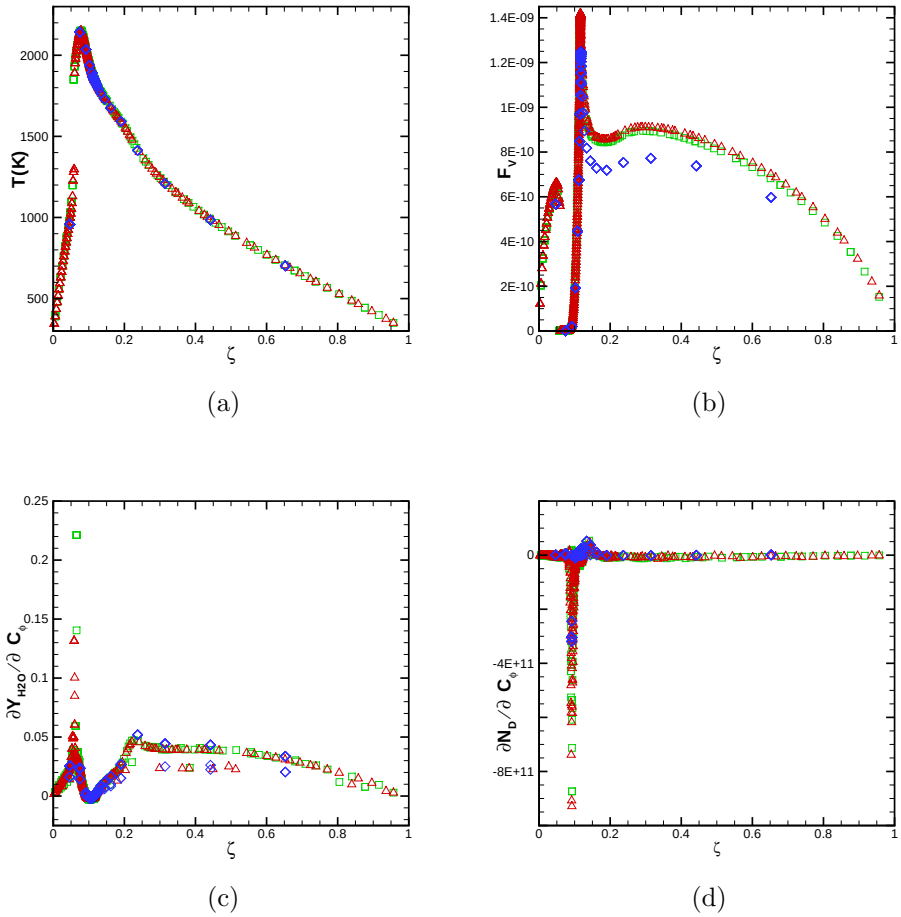

Figure 3.6: Scalar Quantities and Sensitivities for Various Timestep Sizes: △ - 0.005 sec, □ - 0.01 sec, ◇ - 0.1 sec.

The larger timestep of 0.1 seconds showed significant variance from the

baseline, but halving the timestep to 0.005 seconds did not change the resultant plots significantly. This suggests that the initial timestep is sufficient for the purposes of this simulation. Increasing the step size, which decreased simulation run time, produced poor results, which indicates the baseline timestep should not be altered in such a manner. However the longer run time simulation conducted with a smaller step size did not result in enough of a variation in the output to warrant the increased computational cost.

3.3.2 Number of notional particles

Figure 3.7 shows the effect of total number of notional particles used on several scalar quantities and sensitivities. It can be seen that halving the number of notional particles to 512 resulted in less accurate measurements, but doubling the number of particle to 2024 did not significantly enhance the calculations. This trend is readily evident in the scalar plots (Figures 3.7a and 3.7b).

Again, these results indicate the baseline input of 1024 particles sufficiently captures flow sensitivities. The faster runtime resulting from a decreased notional particle count does not outweigh the subsequent inaccuracies, nor does the additional information gained outweigh the longer simulation runtime caused by increasing notional particle count.

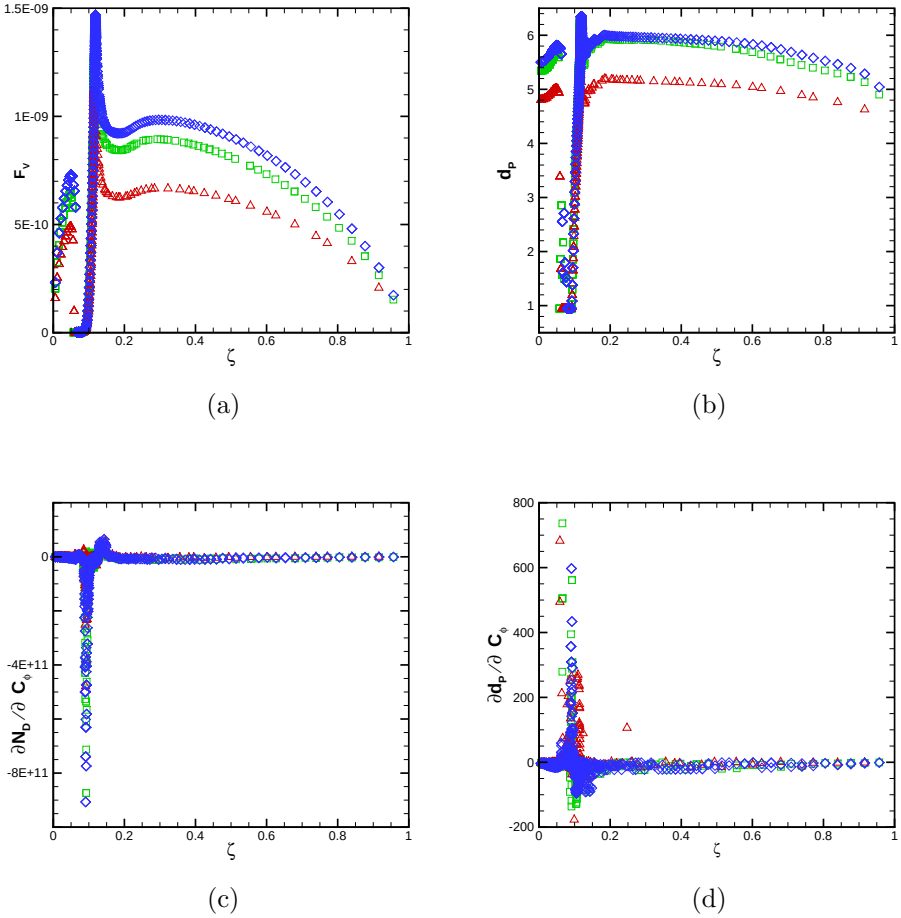

Figure 3.7: Scalar Quantities and Sensitivities for Various Total Number of Notional Particles: △ - 512 particles, □ - 1024 particles, ◇ - 2048 particles.

3.3.3 Mixing time

The mixing timescale τ_{mix} was altered to see its affect on the sensitivities. Increasing the value from 0.02 to 0.1 simulated a slower flow with less mixing. However when mixing in the reactor decreases, eventually there is not enough interaction between the fuel and oxidizer for a reaction to occur; this proved to be the case with the large mixing time scale. Extinction is clearly evident in Figure 3.8b, as the temperature remains around 298 K across all mixture fractions.

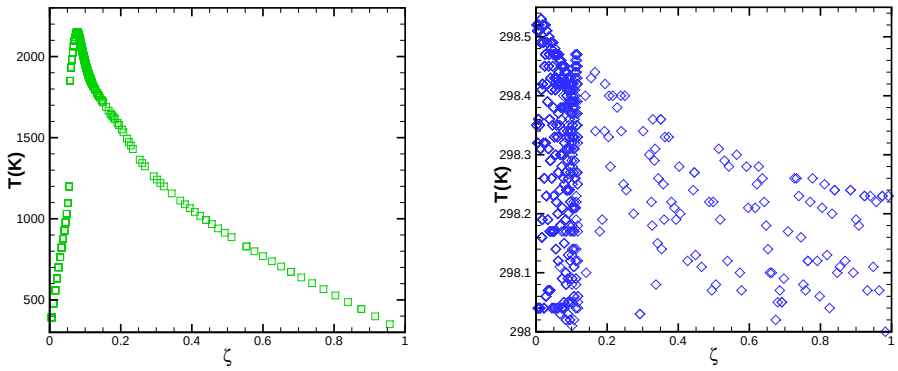

(a) (b)

Figure 3.8: Comparison of (a) Baseline and (b) Large Mixing Time Temperature Profiles.

Going the opposite direction, decreasing the mixing timescale by a factor of 10 resulted in scalar values being more concentrated around the flame core. As can be noted in Figure 3.9, the particle outputs are closely bunched in between ζ=0.05 and 0.15. The faster mixing time resulted in particles

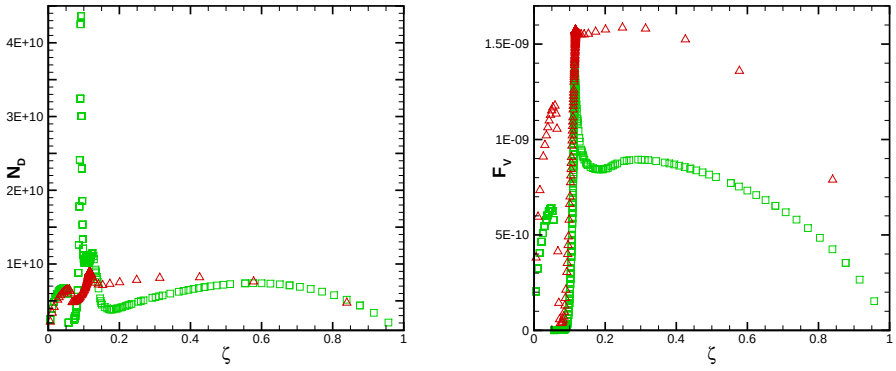

(a) (b)

Figure 3.9: Scalar Quantities at τ_{mix} of □ - 0.02 and △ - 0.002

approaching the steady-state mixture fraction value at a quicker pace. This faster mixing timescale also resulted in a decrease in sensitivity to the mixing model constant as can be seen in Figure 3.10.

3.3.4 Residence time

Increasing the residence time τ_{res} from 0.1 to 1 second significantly altered the scalar profiles and sensitivities. The soot quantity profiles were significantly different from the base case, as can be seen in the volume fraction plot in Figure 3.11. This suggests a strong relationship between soot formation and chemistry, as more reactions would occur the longer particles linger in the reactor. Also lending credence to this idea is the fact that, as in the small mixing time case, particle results are clumped more heavily in the reaction zone between the fuel-lean and fuel-rich boundaries, and the soot quantity

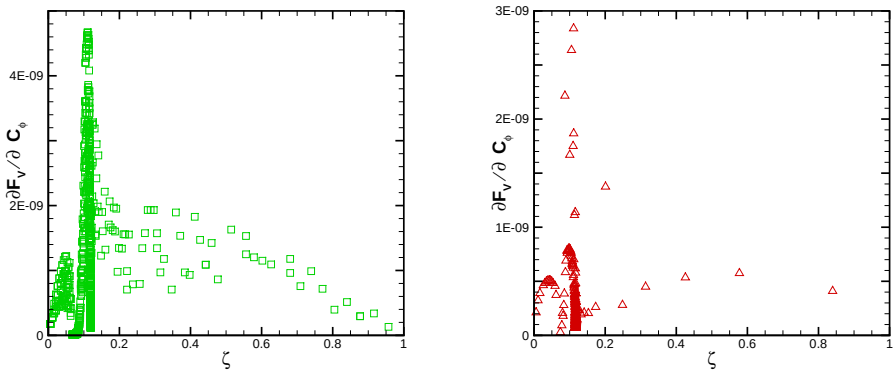

(a) (b)

Figure 3.10: Comparison of (a) Baseline and (b) Small Mixing Time Soot Volume Fraction Sensitivities

sensitivities to mixing decrease. This can be seen in Figure 3.12.

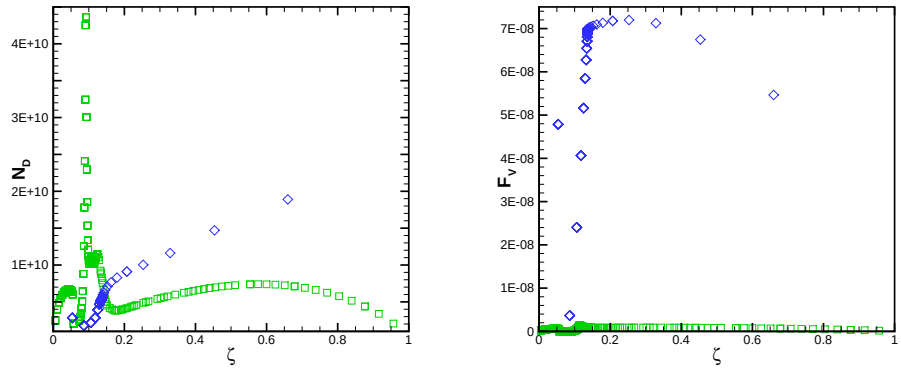

(a) (b)

Figure 3.11: Scalar Quantities at $\boldsymbol{\tau_{res}}$ of □ - 0.1 sec and ◇ - 1.0 sec

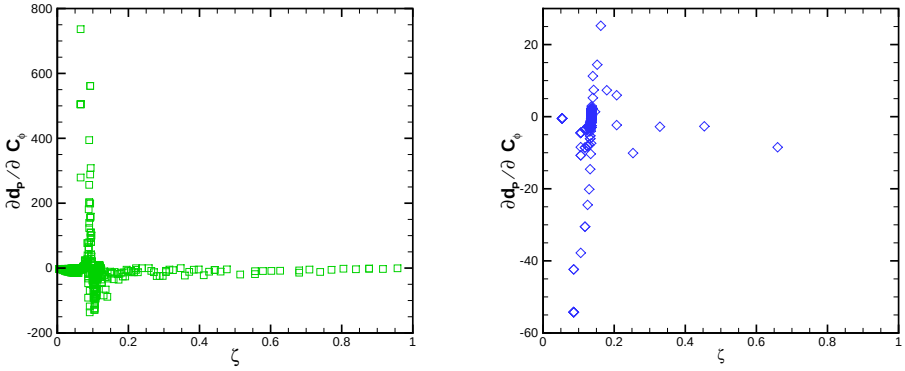

(a) (b)

Figure 3.12: Comparison of (a)Baseline and (b) Large $\boldsymbol{\tau_{res}}$ Sensitivity Profiles

Chapter 4

Conclusions

Sensitivity analysis was performed on a soot model using a PaSR in order to determine the effects of mixing model parameters on soot scalar values. The sensitivities of the mixture fraction $\boldsymbol{\zeta}$ and progress variable $\boldsymbol{C}$ to the mixing model constant $\boldsymbol{C_\phi}$ were calculated; these values were then used to compute the sensitivity of the water mass fraction $\boldsymbol{Y_{H_2O}}$ and soot moments to $\boldsymbol{C_\phi}$.

The results of the simulation were first validated by evaluating the mean mixture fraction sensitivity and a long simulation time case. From the baseline case, it was noted that soot moment sensitivities tended to peak around the stoichiometric mixture fraction $\boldsymbol{\zeta_{st}}$. The fuel-lean and fuel-rich boundaries to the reaction zone were identified using the water mass-fraction sensitivity to mixing model constant. Similarities were noted in the profile shapes of soot volume fraction $\boldsymbol{F_V}$ and particle diameter $\boldsymbol{d_P}$.

Timestep, number of notional particles, mixing timescale $\boldsymbol{\tau_{mix}}$, and residence time $\boldsymbol{\tau_{res}}$ were varied independently to examine their effects on the simulation. It was found that decreasing timestep and particle count resulted in a loss of fidelity in the scalar profiles, but increasing the values did not

add significant information. Variations in timestep and number of notional particles did not significantly alter the sensitivity profiles. Increasing $\boldsymbol{\tau_{mix}}$ resulted in extinction, as not enough mixing occurred for a reaction to be sustained. Decreasing $\boldsymbol{\tau_{mix}}$, however, resulted in a decrease in sensitivity to mixing. The faster mixing rate meant more particles reaching stoichiometric values, increasing in the importance of the chemical processes and decreasing the importance of mixing. Similar trends were noticed when $\boldsymbol{\tau_{res}}$ was increased to lengthen the particles' duration within the reactor. In addition to the decreased sensitivity to mixing and increased number of particles with $\boldsymbol{\zeta}$-values in the reaction zone, scalar profiles were significantly altered.

From these results, it is concluded that the soot model, while exhibiting some sensitivity to the mixing model, is much more susceptible to reaction mechanisms. In both the small $\boldsymbol{\tau_{mix}}$ and large $\boldsymbol{\tau_{res}}$ cases, the increased number of particles reaching stoichiometric values resulted in a decrease in sensitivity to mixing.

Further study could be conducted by performing a similar sensitivity analysis to reaction-related variables, instead of to $\boldsymbol{C_\phi}$. This would further affirm the conclusion that the soot model is more sensitive to the reaction mechanism. Additionally, sensitivity analysis could be performed with other mixing models besides the IEM model to see if the soot model is more sensitive to mixing expressed in a different manner.

Bibliography

[1] S.M. Correa. Turbulence-chemistry interactions in the intermediate regime of premixed combustion. *Combustion and Flame*, 93(1-2):41 – 60, 1993.

[2] Matthias Ihme, Chong M. Cha, and Heinz Pitsch. Prediction of local extinction and re-ignition effects in non-premixed turbulent combustion using a flamelet/progress variable approach. *Proceedings of the Combustion Institute*, 30(1):793 – 800, 2005.

[3] M.E. Mueller, G. Blanquart, and H. Pitsch. Hybrid method of moments for modeling soot formation and growth. *Combustion and Flame*, 156(6):1143 – 1155, 2009.

[4] Michael Edward Mueller, Guillaume Blanquart, and Heinz Pitsch. A joint volume-surface model of soot aggregation with the method of moments. *Proceedings of the Combustion Institute*, 32(1):785 – 792, 2009.

[5] Norbert Peters. *Turbulent Combustion*. Cambridge Monographs on Mechanics. Cambridge University Press, 2000.

[6] Charles D. Pierce and Parviz Moin. Progress-variable approach for large-eddy simulation of non-premixed turbulent combustion. *Journal of Fluid Mechanics*, 504(-1):73–97, 2004.

[7] Zhuyin Ren and Stephen B. Pope. An investigation of the performance of turbulent mixing models. *Combustion and Flame*, 136(1-2):208 – 216, 2004.

[8] Zhuyin Ren and Stephen B. Pope. Sensitivity calculations in pdf particle methods. *Combustion and Flame*, 153(1-2):202 – 215, 2008.

Vita

Nathan Gabriel Wu was born in Austin, Texas. After graduating from Westwood High School, Austin, Texas, he enrolled in the University of Texas at Austin in the fall of 2004, and received the degree of Bachelor of Science in May, 2008. He worked briefly as a staff engineer at Ensoft, Inc. in Austin, Texas, performing analysis on wind turbine foundations before applying to his alma mater for enrollment in their graduate Aerospace Engineering program. He was accepted and began graduate studies in January, 2009.

Permanent address: 11518 Chancellroy Drive
Austin, Texas 78759

This thesis was typeset with LaTeX[†] by the author.

[†]LaTeX is a document preparation system developed by Leslie Lamport as a special version of Donald Knuth's TeX Program.